Temperature Distribution in Lunar Rilles

A. S. ADORJAN*
General Electric Company, Houston, Texas

An analytical investigation on the temperature distribution in lunar rilles is presented. The rille is approximated by an infinite cylindrical cavity whose contour is characterized by a dimensionless nth-order parabolic relation. The surface of the cylinder is irradiated by the sun. The governing equations of the heat balance in the rille are formulated in Fredholm's integral equations of the second kind. A numerical solution method is selected to solve the governing equations by using successive substitution in the form of Neumann's series. The convergence of these series is discussed and a method developed on the solution of the heat balance equations, numerical examples are given to illustrate the temperature distribution in rilles with different width to depth ratios at various solar elevation angles. The temperature of the shadowed surface of the rille varies along the width. To account for the effect of the thermal inertia of the lunar soil on the surface temperatures, an approximate method is given, by utilizing the concept of surface sources, for the correction of the temperatures of the shadowed surfaces.

Nomenclature

A = surface area, ft²
a = D/h, aspect ratio of rille, width/depth
F_{ij} = form factor relating A_i and A_j
J = radiosity at an arbitrary location, Btu/hr-ft²
K_{ij} = kernel of Fredholm's integral equation or normalized form factor in the heat balance equations
n = even power of parabolic contour relation
q = local incident heat flux, Btu/hr-ft²
S = solar constant, 442 Btu/hr-ft²
T = radiation equilibrium temperature, °R
α,ϵ = absorptivity and emissivity of lunar soil
γ = thermal inertia of lunar soil, 750 cm²-sec$^{1/2}$-°C/cal
δ = solar elevation angle
η,ξ = dimensionless depth and width of rille
λ = parameter of the integral equation
σ = Stefan-Boltzmann constant, 0.1714 × 10^{-8} Btu/hr-ft²-°R⁴
ϕ = inclination angle to surface normal

Subscripts

1,2 = sunlit and shadowed regions of the rille
s = source

Introduction

FOR future lunar landings, lunar rilles present significant scientific interest. High-resolution Lunar Orbiter V photographs of the rille Rima Hadley,[1] for example, indicate fresh exposures of rocks on the walls of the rille that may answer some of the questions concerning the geological history of the moon. Significant analytical effort has been spent in recent years on the thermal analysis of other topographical features, for example, lunar craters. In general, the heat balance for this type of problem can be formulated in Fredholm's integral equations of the second kind. In an earlier paper, Adorjan[2] gave a rigorous mathematical solution of the Fredholm equations in closed form for lunar craters by using spherical approximation for the surface contour. The same results were obtained by Buhl[3] by mathematical induction. For lunar rilles, the heat balance equations do not lend themselves to easy closed form analytical solutions. Consequently, in the present study a numerical method was adapted to obtain the temperature distribution in lunar rilles.

Presented as Paper 70-819 at the AIAA 5th Thermophysics Conference, Los Angeles, Calif., June 29–July 1, 1970; submitted August 17, 1970; revision received February 19, 1971. The study was conducted for NASA by General Electric under Contract NASw-410.

* Consulting Engineer. Member AIAA.

Analysis

The lunar rilles in this study are approximated by infinite cylindrical cavities. The contour of the cylinder is characterized by a dimensionless nth-order parabolic relation,

$$\eta = (2/a)(\xi^n - 1) \tag{1}$$

where ξ and η are the dimensionless width and depth respectively, a is the aspect ratio of the cavity (the ratio of the width to the maximum depth) and $n = 2, 4, 6, 8, \ldots$ are even integers which define the shape of the contour. The change of shape as a function of n is illustrated in Fig. 1. The contour approaches a rectangle if n approaches infinity. The aspect ratio is arbitrary. The surface of the rille is illuminated by a collimated beam, such as the sun. Figure 2 depicts the thermal and geometrical conditions used in the analysis.

To determine the temperature distribution in the rille, first the governing equations of the heat balance are defined in a set of integral equations. Independent of the depth of the rille, the total incident solar radiation is identical for all rilles with the same width at their openings. By energy consideration, the total emitted radiation must also be the same. Consequently, heat emission from deep rilles may occur at higher surface temperatures to compensate for the decrease of the form factor from the cavity toward the deep space.

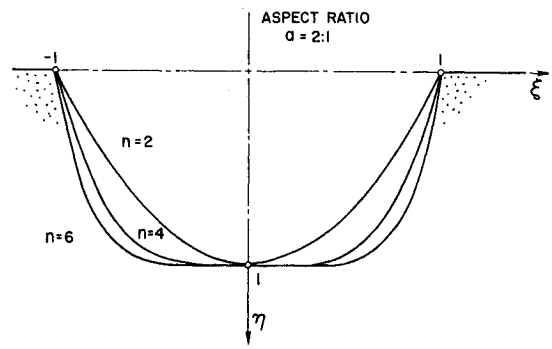

Fig. 1 Parabolic approximation of the contours of lunar rilles.

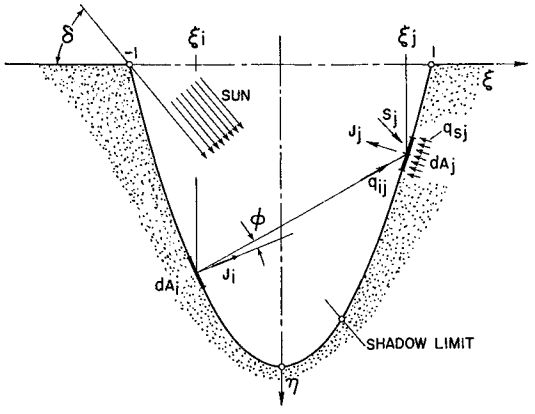

Fig. 2 Model of lunar rilles.

To simplify the analysis, it is assumed that the emissivity of the surface is unity (corresponding closely to the experimental data) and that the absorptivity is also unity instead of the usual 0.93. Uncertainties of local albedo values and gross assumptions on the shape of the surface contour may introduce larger errors than the second assumption. In addition, reabsorption from the first and higher order reflections of the incident radiation may result in an effective absorptivity significantly higher than 0.93.

In Fig. 2 the incident heat flux at A_j from the sun and subsurface sources is

$$q_i = S_j + q_{sj} \tag{2}$$

and radiation leaving surface dA_i which is absorbed at surface dA_j is

$$dA_j q_{ij} = dA_i dF_{ij} J_i \tag{3}$$

By utilizing the reciprocity relation and the expression for the diffuse form factor, $dF_{ji} = K_{ji}dA_i$, the radiosity at A_j can be expressed as the sum of the incident heat flux and the contribution of radiation originated from all dA_i elements.

Then the radiosity at A_j is

$$J_j = q_j + \int_A K_{ji} J_i dA_i \tag{4}$$

This relation is Fredholm's integral equation of the second kind, which, in mathematical notation is

$$y(x) = f(x) + \lambda \int_a^b K(x,t)y(t)dt \tag{5}$$

where $y(x)$ is the unknown function (here the radiosity of the surface), $f(x)$ is a given function (incident radiation and heat source at the surface), $K(x,t)$ is the kernel of the integral equation (normalized form factor, K_{ji}), and λ is a given parameter. Solution methods for these types of equations are quite complex, except for a few special cases.[4]

The radiosities of the sunlit and shadowed regions, respectively, are

$$J_{1j} = q_{1j} + \lambda_1 \int_{A_1} K_{ji} J_{1i} dA_i + \lambda_2 \int_{A_2} K_{ji} J_{2i} dA_i \tag{6}$$

and

$$J_{2j} = q_{2j} + \lambda_1 \int_{A_1} K_{ji} J_{1i} dA_i + \lambda_2 \int_{A_2} K_{ji} J_{2i} dA_i \tag{7}$$

The foregoing equations are the governing relations for a black, partially shadowed cavity with arbitrary shape. In general, the four kernels are different, being functions of the geometry of the cavity and the relative size and location of the shadow. These kernels may cause difficulties in the solution of Eq. (5).

The general expression of the form factor for infinite parallel strips,[5] by using the notation of Fig. 2, is

$$dF_{ij} = \tfrac{1}{2} d(\sin\phi) \tag{8}$$

Consequently, the normalized form factor for the infinite rille can be written as

$$K_{ij} = dF_{ij}/d\xi_j = \tfrac{1}{2}\, d(\sin\phi)/d\xi_j \tag{9}$$

By expressing $\sin\phi$ in terms of the dimensionless rectangular coordinates, according to the geometrical relations given in Fig. 2, K_{ij} can be obtained by differentiation as

$$K_{ij} = \tfrac{1}{4}(C_2/C_1^{1/2}C_3^{1/2} - C_4 C_1^{1/2}/C_3^{3/2}) \tag{10}$$

where

$$C_1 = C_{11} + C_{12}$$

$$C_{11} = [4n\xi_i^{n-1}(\xi_i^n - \xi_j^n) + a^2(\xi_i - \xi_j)]^2/(4n^2\xi_i^{2n-2} + a^2)^2$$

$$C_{12} = [8n^2\xi_i^{2n-2}(\xi_i^n - \xi_j^n) + 2na^2\xi_i^{n-1}(\xi_i - \xi_j)]^2/(4an^2\xi_i^{2n-2} + a^3)^2$$

$$C_2 = -2C_{11}^{1/2}\frac{4n^2\xi_i^{n-1}\xi_j^{n-1} + a^2}{4n^2\xi_i^{2n-2} + a^2} - 4C_{12}^{1/2}\frac{4n^3\xi_i^{2n-2}\xi_j^{n-1} + na^2\xi_i^{n-1}}{4an^2\xi_i^{2n-2} + a^3}$$

$$C_3 = (\xi_i - \xi_j)^2 + 4(\xi_i^n - \xi_j^n)^2/a^2$$

$$C_4 = 2(\xi_j - \xi_i) - 8n(\xi_i^n - \xi_j^n)\xi_j^{n-1}/a^2$$

By using the same notation, the incident heat flux (solar radiation and subsurface source) at A_j is

$$q_j = S[\cos\delta/(1 + a^2/4n^2\xi_j^{2n-2})^{1/2} + \sin\delta/(1 + 4n^2\xi_j^{2n-2}/a^2)^{1/2}] + q_s \tag{11}$$

where S is the solar constant, δ is the solar elevation angle, and q_s is the subsurface source.

Method of Solution

Substituting Eqs. (10) and (11) into Eqs. (6) and (7) the governing equations for the radiosity and the temperature of shadowed infinite rilles can be obtained. In order to solve the resulting integral equations, the method of successive substitution will be applied by using the iterated kernels. The successive substitution method yields the solution in an infinite series, known as Neumann's series.[6] The sum of the series can be computed for the desired accuracy if the series is absolutely and uniformly convergent;

$$y(x) = f(x) + \lambda \int_a^b K(x,t)f(t)dt + \lambda^2 \int_a^b K(x,t) \int_a^b K(t,t_1)f(t_1)dt_1dt + \lambda^3 \int_a^b K(x,t) \int_a^b K(t,t_1) \int_a^b K(t_1,t_2)\, f(t_2)dt_2dt_1dt + \lambda^4 \ldots + R_n(x) \tag{12}$$

The first term on the right-hand side of Eq. (12) is the given function, *i.e.*, the incident radiation and the heat source at the surface, expressed by Eq. (11). The subsequent terms account for the radiative interchange in the cavity. The kernel in these terms is given in Eq. (10) and t is a dummy variable. Figure 1 illustrates the coordinate system for the analysis. The dimensionless independent variable is ξ corresponding to the variable x. Similarly, the limits of integration, a and b are replaced by -1 and 1. $R_n(x)$ is the remainder of the series.

To perform the integration indicated in Eq. (12) by numerical technique the ξ axis is subdivided into equal intervals. The number of intervals influences significantly the accuracy of the solution. In general, low sun angles, at which the rille is partially shadowed, require high number of subdivision. This can be explained by the great sensitivity of the surface

temperature at low radiosities. The sensitivity of the surface, as derived from the blackbody relation, $J = \sigma T^4$, is

$$dT/dJ = (\sigma^{3/4}/4)J^{-3/4} \quad (13)$$

Furthermore, low aspect ratios also require high number of subdivisions.

Another consideration in the numerical solution is the number of terms to be taken on the right-hand side of Eq. (12) in order to obtain convergence. For large aspect ratios, a few terms are sufficient. Decreasing a requires increasing number of terms. At $a = 2$ approximately 10 terms are required. For lower aspect ratios such a great number of terms might be necessary that computer storage can be exceeded. It was observed during this study that the higher order terms can be approximated by a geometrical series. Consequently, the summation of the Neumann series was terminated at a certain number of terms and the remainder was computed by approximating the sum of the series. Aspect ratios of $a \leq 1$ may result in alternating terms in the series. In this case the series has to be separated into individual, uniformly converging series in order to be able to apply the geometrical series approximation method. Further discussion of this method can be found in the Appendix.

To obtain realistic surface temperature for the shadowed region of the rille, the following correction is made. Equation (12) indicates that for the case of $q_s = 0$, the temperature of the shadowed region of the rille approaches 0°R when the solar elevation angle is zero, i.e., between sunset and sunrise points. This is not in agreement with lunar surface temperature data obtained by experimental methods.[7,8] In effect, the minimum lunar surface temperature is not lower than ~170°R, because of the thermal inertia of the lunar soil. During the lunar day, the thermal energy penetrates into the soil and at night, it reverses the direction and flows toward the outside. As an approximation, the outward flowing heat can be considered as a surface source in the heat balance equation for lunar night and lunar shadow conditions. Taking $T = 170$°R as the minimum "level," corresponding to a thermal inertia of $\gamma = 750$ cm²-sec$^{1/2}$-°C/cal, the equivalent surface source is

$$q_s = \sigma T_s^4 = 1.4 \text{ Btu/hr-ft}^2$$

It can be shown that by carrying on the source q_s in the computation of the rille temperatures in the sunlit region, the error introduced by the approximation is less than 1°R for a solar elevation angle of 90° and a 2:1 aspect ratio rille. The results of the error analysis are given in the Appendix.

Discussion of Results

The surface temperatures in the rilles are obtained from the solution of the radiosity equations, Eqs. (5) and (6) by using the Stefan-Boltzmann relation, $J = \sigma T^4$. Figure 3a illustrates the temperature distribution in a rille with aspect ratio $a = 1$ for 45° and 90° sun angles. The results are compared for contour shapes represented by $n = 2$ and $n = 4$. Discontinuities in the 45° temperature profiles indicate the shadow limits. The maximum temperature in a $n = 1$ aspect ratio rille (or crevice) is approximately 350°F for a second order parabolic contour. In comparison, the black-body equilibrium temperature of the lunar plain at $\delta = 90°$ is approximately 250°F. For $n = 4$ the maximum temperature is lower, but it is more widely distributed along the width of the rille. In general, the shadow temperatures are lower for the $n = 2$ case than for the $n = 4$ case, which can be explained by energy considerations. For the $n = 2$ case, the sunlit region is wider than for the $n = 4$ case; however, the temperatures are approximately the same. The energy received is identical for both cases; consequently, the shadow temperatures are lower for the $n = 2$ case. For Figs. 3a and

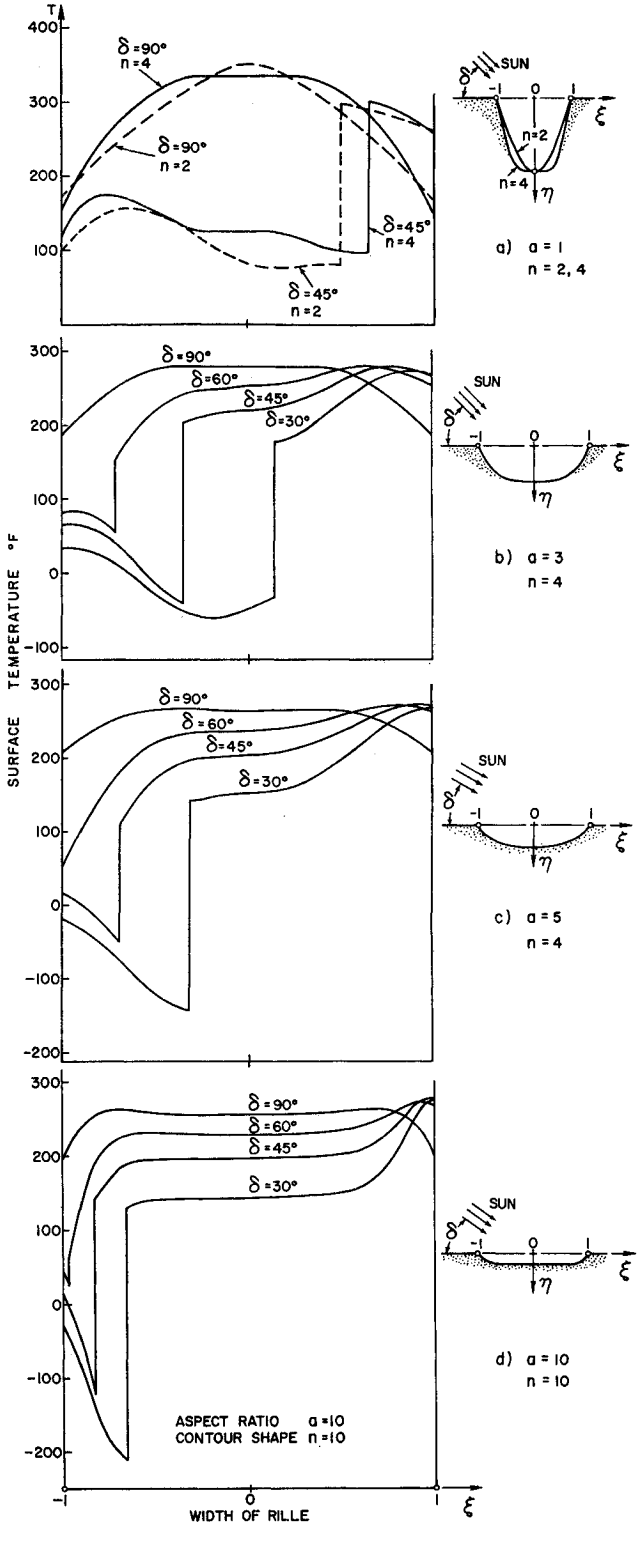

Fig. 3 The effect of contour shape and aspect ratio on the temperature distribution in lunar rilles.

5b it is assumed that the rille has a north-south orientation. Temperature distribution for arbitrary orientation can be easily obtained by using the appropriate transformation for the solar load and by redefining the shadow limit. Furthermore, it is also assumed that the surface of the contour cylinder is parallel to the level lunar plain. Figures 3 and 3c give the temperature distribution in $a = 3$ and $a = 5$ aspect ratio craters respectively. The lunar rille Rima Hadley, which is approximately 1.5 km wide and 300–500 m deep represents this aspect ratio range.[1] The contour shapes correspond to

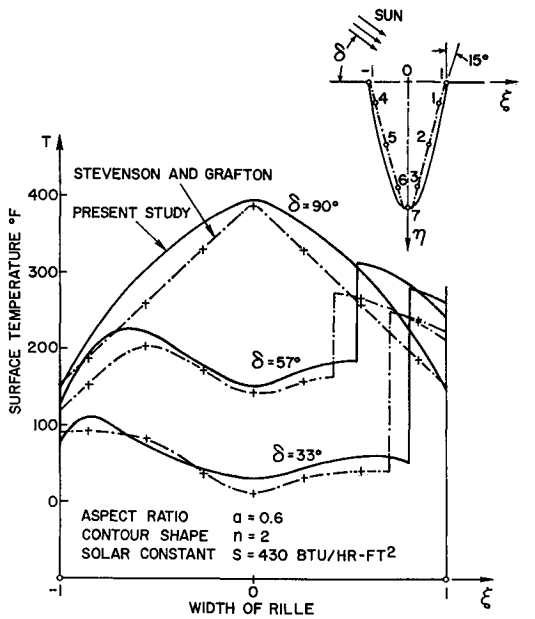

Fig. 4 Comparison of the results of Stevenson and Grafton with the present study.

$n = 4$ for both aspect ratios. It can be seen that the maximum temperature is not at $\delta = 90°$ but at approximately $\delta = 45°$. Figure 3d represents a shallow lunar rille, with an aspect ratio of $a = 10$ and a contour shape corresponding to $n = 10$. Again, the maximum temperature of the rille occurs at approximately 45° sun angle. At 90° sun angle, the temperature profile has two maxima at around $\xi = \pm 0.7$. The temperature in the middle of the rille at $\xi = 0$ is a few degrees lower than the maximum.

The results of an earlier investigation which was performed by Stevenson and Grafton[9] are compared in Fig. 4 with those predicted by the present study. The aforementioned investigators determined the temperatures in an infinite, trapezoidal rille (or fissure). They employed radiosity network in their solution and used seven surface nodes as illustrated in Fig. 4. The basic assumptions are the same as in the present study (blackbody approach, infinite long rille). Thermal inertia of the soil is not considered. The solar constant used is $S = 430$ Btu/hr-ft² instead of 442. For easier comparison, the results by the present method are also given for $S = 430$ Btu/hr-ft². The trapezoidal contour is approximated by a $a = 0.6$ aspect ratio rille with a second-order parabolic relation. The comparison indicates a good qualitative agreement between the two studies. Stevenson and Grafton gave temperature results only at the 7 nodal midpoints for 33°, 57°, and 90° solar elevation angles. The curve for 33° sun angle indicates, especially in the vicinity of $\xi = -1$, that the number of points is insufficient to clearly define the interconnecting temperature curve. Figure 5a illustrates the dependence of the maximum rille temperatures as a function of the aspect ratio. It can be seen that the maximum temperature in the rille rises sharply at aspect ratios less than approximately $a = 1$. The contour shape corresponds to a second-order ($n = 2$) parabolic relation. For this profile the maximum temperature occurs at 90° and at $\xi = 0$. At increasing aspect ratios the maximum temperature approaches asymptotically the equilibrium temperature of the lunar plain ($a \to \infty$). The effect of thermal inertia on the maximum temperature profile is not significant. (See Appendix for results of error analysis.)

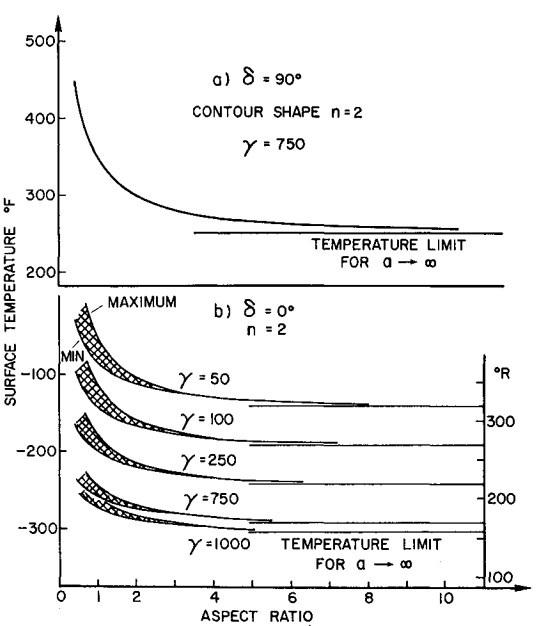

Fig. 5 Maximum T's and ragnes of T at lunar sunrise, as functions of aspect ratio.

Table 1 Terms in Neumann's series for rilles with $a = 10$ and $a = 1$, at $\xi = -1$

m	$a = 10, n = 8, \delta = 40°$ Q_m	P_m	$a = 1, n = 2, \delta = 45°$ Q_m
1	63.82061386		119.3893
		0.053	
2	3.35453844		2.2261
		0.144	
3	0.48314667		27.1955
		0.082	
4	0.03939493		2.2083
		0.105	
5	0.00415594		8.1543
		0.092	
6	0.00038115		1.1993
		0.098	
7	0.00003744		2.5551
		0.095	
8	0.00000355		0.5328
		0.096	
9	0.00000034		0.8132
10			0.2157
11			0.2619
12			0.0829
13			0.0852
14			0.0309
15			0.0280

The behavior of the range of rille temperatures at lunar sunrise is given in Fig. 5b. The effect of thermal inertia on these temperatures is very pronounced. The limiting temperatures for $a \to \infty$ are based on Sinton's[10] data. Because of the absence of solar radiation, the attitude and orientation of the rille can be arbitrary. The cavity effect of the rille is quite significant; at an aspect ratio of $a = 3$ the minimum surface temperature of the rille exceeds the temperature of the lunar plain ($a \to \infty$) by 10°F at $\gamma = 750$ cm²-sec$^{1/2}$-°C/cal and by 19°F at $\gamma = 50$ cm²-sec$^{1/2}$-°C/cal. In an earlier study, Buhl[11] suggested the cavity effect to explain the thermal anomalies (hot spots) observed on the moon by Saari and Shorthill.[12] During lunation the temperature anomalies of some craters are of the order of 10°–20°K, although during eclipse the hot spot may exceed the temperature of the surroundings by as much as 50°K (Crater Tycho). Buhl showed that for spherical geometry, diameter to depth ratios of $a < 1$ would be necessary (for a hemisphere $a = 2$) to produce a 50°K anomaly. According to Fig. 5b a rille with an aspect ratio of $a = 0.5$ would give a temperature excess of 50°K at $\gamma = 750$ cm²-sec$^{1/2}$-°C/cal. The excess is significantly higher

at lower thermal inertia values. Another explanation of the thermal anomalies is the significant decrease in the value of the thermal inertia in craters, rilles and around rough surfaces. Reference 1 shows a high-resolution view of a portion of the rille Rima Hadley, obtained from a photograph taken by Lunar Orbiter V. The picture clearly indicates abundant rocks on the slope of the rille and a ledge of bedrock on one of the walls. Sample measurements of Apollo 12 lunar samples[13] clearly indicate the large difference in the thermal inertia of lunar rocks and dust. According to these measurements the thermal inertia of lunar rocks and dust are around 20 and 950 cm^2-sec$^{1/2}$-°C/cal, respectively, at room temperature. Even if the walls of the rilles are composed of an aggregate of dust and rocks of different sizes on the surface and directly underneath, instead of solid rocks, the value of the effective thermal inertia may decrease significantly. For example, according to Fig. 5b, a decrease of γ from 750 to 100 cm^2-sec$^{1/2}$-°C/cal would result in a temperature rise of 100°F for flat lunar plain. The cavity effect of the rille enhances the temperature rise even further. The relative contribution of the cavity effect and changes in thermal inertia to the thermal anomalies could be explained only after experimental data become available. Infrared imaging from lunar orbit or preferably from the lunar surface itself would be one of the methods to clarify the nature and causes of lunar hot spots. In addition analytical predictions of temperature distribution in rilles, craters and in other topographical features could be verified experimentally by the preceding method if it becomes available in the future.

Appendix

In the numerical solution of the heat balance equation by Neumann's series, the convergence of the series is an important factor. Series with slow convergence may require too many terms to achieve the necessary accuracy. For large aspect ratios, it was observed that a few terms are sufficient. Furthermore, the series is uniformly convergent; thus the geometrical series approximation can be used directly to compute the remainders.

Table 2 Odd and even terms in Neumann's series for $a = 1.0$

m	Q_m	P_m	Z_m
1	119.3893		
		0.2278	
3	27.1955		0.7597
		0.2998	
5	8.1543		0.9569
		0.3133	
7	2.5551		0.9845
		0.3183	
9	0.8132		0.9882
		0.3221	
11	0.2619		0.9896
		0.3255	
13	0.0852		0.9909
		0.3284	
15	0.0280		
2	2.2261		
		0.9920	
4	2.2083		1.8267
		0.5431	
6	1.1993		1.2223
		0.4443	
8	0.5328		1.0974
		0.4049	
10	0.2157		1.0533
		0.3844	
12	0.0829		1.0328
		0.3722	
14	0.0309		

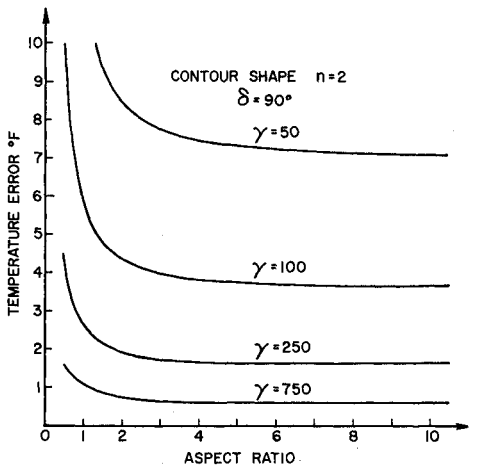

Fig. 6 Errors in maximum temperatures due to the thermal inertia approximation.

The second column of Table 1 gives the terms of Neumann's series for an $a = 10$ aspect ratio rille at $\delta = 40°$ solar elevation angle at the location of $\xi = -1$. The contour shape is characterized by $n = 8$. The subscript m denotes the individual terms; $m = 1$ corresponds to the second term on the right-hand side of Eq. (12). P is the quotient of the series computed by the relation $P_m = Q_{m+1}/Q_m$.

The quotient for higher order terms is 0.096; thus the remainder can be computed by replacing the remaining terms by an infinite geometrical series whose sum can be obtained by the relation $R_k = Q_k/(1 - P_k)$ where subscript k indicates the first term in the geometrical series approximation.

The result of the summation up to $m = 9$ is

$$Q = \sum_{m=1}^{9} Q_m = 67.702 \text{ Btu/hr-ft}^2$$

The remainder does not have a significant figure up to the third place after the decimal point

$$R_{10} = 0.000$$

The first term in Neumann's series is

$$q_s = 1.431 \text{ Btu/hr-ft}^2$$

Thus the radiosity at $\xi = -1$ can be obtained as

$$J = q_s + Q + R_{10} = 69.133 \text{ Btu/hr-ft}^2$$

Aspect ratios of approximately $a \leq 1$ may result in series which are not uniformly convergent in the higher order terms. Consequently, direct approximation by geometric progression is not feasible. The last column of Table 1 shows the terms of Neumann's series for an $a = 1$ aspect ratio rille at a sun angle of $\delta = 45°$ at a location of $\xi = -1$. The contour is a second-order parabola.

It can be seen that the terms of the series alternate. Further inspection of the series reveals, however, that it can be separated into two series according to the odd and even terms, each of which is uniformly convergent. Table 2 gives these series. Z denotes the quotient of the quotients of the series, which measures the convergence of the quotients of Q, thus indicating how rapidly Q approaches toward a geometrical progression.

The result of summation of the series up to the 14th term is

$$Q = \sum_{m=1}^{14} Q_m = 164.9506 \text{ Btu/hr-ft}^2$$

The remainder is computed by approximating the terms of the series higher than $m = 14$ by two geometrical progres-

sions. The sum of the summation of the two series gives

$$R_{15} = 0.1780 \text{ Btu/hr-ft}^2$$

In Neumann's series the first term is

$$q_s = 1.4315 \text{ Btu/hr-ft}^2$$

Thus the radiosity at $\xi = -1$ can be obtained as

$$J = q_s + Q + R_{15} = 166.5602 \text{ Btu/hr-ft}^2$$

In this study, a method is presented for temperature correction to account for the effect of the thermal inertia of the lunar soil. This correction, which appears as an additive term in the heat balance equations, is the most significant for shadow temperatures. In reality, the thermal inertia effect can be considered as a source for shadow and lunar nighttime conditions and a sink for most of the lunar day. Consequently, the approximation used in this study results in positive temperature errors at higher solar elevation angles. Figure 6 gives these errors at lunar noon ($\delta = 90°$). The reference temperature (zero error) for the error curves corresponds to isolation conditions, i.e., to $\gamma = \infty$. The actual error is somewhat higher, because of the sink effect due to the thermal inertia. To obtain an exact solution for the thermal inertia effects, the simultaneous solution of the heat diffusion equation and the integral equations of the heat balance of the lunar rille is required.

References

[1] Hess, W. et al., "The Exploration of the Moon," *Scientific American*, Vol. 221, Oct. 1969, pp. 54-72.

[2] Adorjan, A. S., "Temperature Distribution in Shadowed Lunar Craters," *Journal of Spacecraft and Rockets*, Vol. 7, No. 3, March 1970, pp. 378-380.

[3] Buhl, D. et al., "Reradiation and Thermal Emission from Illuminated Craters on the Lunar Surface," *Journal of Geophysical Research*, Vol. 73, Aug. 1968, pp. 5281-5295.

[4] Volterra, V., *Leçons sur les Equations Intégrales et les Equations Intégrodifférentielles*, Gautier-Villars, Paris, 1913.

[5] Howell, J. R. and Siegel, R., *Thermal Radiation Heat Transfer*, Vol. 2, NASA SP-164, 1969, Chap. 2, p. 17.

[6] Courant, R. and Hilbert, D., *Methods of Mathematical Physics*, Interscience, New York, 1966, Chap. 3, pp. 140-142.

[7] Lucas, J. W. et al., "Lunar Temperatures and Thermal Characteristics," *Surveyor III Mission Report*, Pt. II, TR 32-1177, June 1967, Jet Propulsion Lab., Pasadena, Calif., pp. 155-188.

[8] Lucas, J. W. et al., "Lunar Surface Temperatures and Thermal Characteristics," *Surveyor V Mission Report*, Pt. II, TR 32-1246, Nov. 1967, Jet Propulsion Lab., Pasadena, Calif., pp. 89-113.

[9] Stevenson, J. A. and Grafton, J. C., "Lunar Temperature Environment," *Proceedings of the Institute of Environmental Sciences*, April 1960, Los Angeles Calif., pp. 233-242.

[10] Sinton, W. M., "Temperatures on the Lunar Surface," *Physics and Astronomy of the Moon*, edited by Z. Kopal, Academic Press, New York, 1962, Chap. 11, pp. 407-428.

[11] Buhl, D. et al., "Anomalous Cooling of a Cratered Lunar Surface," *Journal of Geophysical Research*, Vol. 73, Dec. 1968, pp. 7593-7608.

[12] Saari, J. M. and Shorthill, R. W., "Isotherms of Crater Regions on the Illuminated and Eclipsed Moon," *Icarus*, Vol. 2, Aug. 1963, pp. 115-136.

[13] Robie, R. A. et al., "Specific Heats of Lunar Surface Materials from 90 to 350 Degrees Kelvin," *Science*, Vol. 167, Jan. 1970, pp. 749-750.